Crystal field of Dy implanted in Ag obtained by Mössbauer spectroscopy

P. J. Kikkert and L. Niesen
Laboratorium voor Algemene Natuurkunde, University of Groningen, The Netherlands
(Received 3 June 1980)

The magnetic field dependence of the hyperfine interaction of ^{161}Dy impurities in Ag has been studied in external fields up to 3.2 T by means of Mössbauer spectroscopy. ^{161}Dy was introduced into a single crystal of Ag by means of low-temperature implantation. From the measurements we can determine the parameters of the cubic crystalline electric field (CEF) acting on the Dy nuclei: $A_4\langle r^4\rangle = -13.5 \pm 4.5$ K and $A_6\langle r^6\rangle = +5.7 \pm 0.3$ K. These results seem to be at variance with those of other methods. However, we will show that the above CEF parameters can account for the other experimental results as well. It may be concluded that in this case Mössbauer spectroscopy is probably the only method to determine the CEF parameters $A_4\langle r^4\rangle$ and $A_6\langle r^6\rangle$ with reasonable accuracy.

I. INTRODUCTION

Present-day interest in low-temperature magnetic properties of rare-earth ions in cubic metallic environments has led to a number of experiments in which various techniques have been used to determine the crystalline electric field (CEF) that plays an important role in these systems (e.g., magnetic susceptibility, specific-heat measurements, inelastic neutron scattering[1–4]). For an accurate determination single crystals of dilute alloys have to be grown in most of these cases. Generally, low solubility hampers the formation of such alloys.

In this paper it will be shown that in those cases Mössbauer spectroscopy on low-temperature-implanted radioactive ions is a useful tool for studying the CEF. As a host we chose Ag, because a number of techniques have been used to determine the CEF parameters of Dy*Ag*[1–3,5,6] with a reasonable accuracy, presenting a test case for our method. From a combination of dc-susceptibility and electron-spin-resonance data[2] it follows that the ground state is a Γ_7 doublet separated from a Γ_8 excited quartet by $\Delta = 11.5 \pm 1.0$ K with an overall multiplet splitting of 160 ± 25 K.

In this paper the hyperfine interaction as found from our Mössbauer-effect measurements is analyzed in terms of the CEF acting on the rare-earth electron spin. Experimental conditions for the accurate determination of the CEF parameters were chosen in such a way that only the lowest electronic state was populated. In this way the influence of relaxation between electronic levels was eliminated and the hyperfine interaction measures directly the moments $\langle J_z\rangle$ and $\langle J_z^2\rangle$ of the electronic ground state as a function of the external magnetic field.

We find the same separation $\Delta = 11.1 \pm 1.1$ K but a much smaller overall splitting (55 K), corresponding to a set of CEF parameters quite different from that found earlier. As will be discussed, all the other experimental results can be explained with this smaller overall splitting, taking into account the concentration inaccuracy.

II. THEORY

In the presence of a magnetic field the most general operator equivalent potential with cubic point symmetry within a manifold of angular momentum J composed of f-electron wave functions may be written in the form[7,8]

$$H = -\tfrac{2}{3}A_4\langle r^4\rangle\beta_J(O_4^0 - 20\sqrt{2}O_4^3) + \tfrac{16}{9}A_6\langle r^6\rangle\gamma_J(O_6^0 + \tfrac{35}{4}\sqrt{2}O_6^3 + \tfrac{77}{8}O_6^6) + g_J\mu_B\vec{B}\cdot\vec{J} \quad (1)$$

with the $\langle 111\rangle$ direction as a three-fold quantization axis. (There is some confusion about the signs of the coefficients of O_4^3 and O_6^3. Here we chose the axes as in Hutchings.[7] Changing the sign corresponds to a rotation of π around the three-fold axis.) $\langle r^4\rangle$ and $\langle r^6\rangle$ are radial integrals, the O_n^m are the so-called operator equivalents, and β_J and γ_J are multiplicative factors as given in Ref. 8.

The coefficients $A_4\langle r^4\rangle$ and $A_6\langle r^6\rangle$ can be calculated if the influence of the environment is approximated by point charges on the fcc lattice, but since the contribution of the conduction electrons, which play an important role in these systems, cannot be calculated, it is customary to regard $A_4\langle r^4\rangle$ and $A_6\langle r^6\rangle$ as parameters to be determined by experiment.

In the case of Dy($^6H_{15/2}$) the qualitative effect of the cubic field Hamiltonian is a splitting of the lowest J multiplet into two doublets (Γ_6 and Γ_7) and three quartets ($\Gamma_8^{(1)}$, $\Gamma_8^{(2)}$, and $\Gamma_8^{(3)}$). In the presence of an external magnetic field these levels are mixed by the Zeeman interaction and any degeneracy is removed.

Because the hyperfine interaction is small compared to the differences between the electronic energy levels, we can use first-order perturbation theory to obtain the magnetic and electric part of the $4f$ contribution to the hyperfine interaction in a certain electronic state[9]:

$$H_M = -g_N \mu_N B_{\rm hf} I_z \ , \tag{2a}$$

with

$$B_{\rm hf} = \frac{\langle J_z \rangle}{J} B_{\rm hf}(\max) = R_M B_{\rm hf}(\max) \ ; \tag{2b}$$

$$H_Q = \frac{e^2 q_{4f} Q}{4I(2(-1)} [3I_z^2 - I(I+1)] \ , \tag{3a}$$

with

$$q_{4f} = \frac{3\langle J_z^2 \rangle - J(J+1)}{3J^2 - J(J+1)} q_{4f}(\max) = R_Q q_{4f}(\max) \ . \tag{3b}$$

In these expressions $B_{\rm hf}(\max)$ and $q_{4f}(\max)$ are the hyperfine field and electric field gradient, respectively, when the $4f$ contribution is maximal ($\langle J_z \rangle = J$). For the case of Dy their values are well known.[9–11] From our low-temperature Mössbauer experiments we can obtain the ratios R_M and R_Q in the electronic ground state as a function of the external magnetic field. On the other hand, by diagonalizing Eq. (1) we can find values for $\langle J_z \rangle$ and $\langle J_z^2 \rangle$ [or, using Eqs. (2b) and (3b) for R_M and R_Q] in terms of the parameters $A_4\langle r^4 \rangle$ and $A_6\langle r^6 \rangle$. These parameters can now be adjusted so as to obtain a least-squares fit to the measured R_M and R_Q.

If not only the lowest electronic level is populated, relaxation phenomena will be present. These can be treated using the rate-equation method,[12] described in detail by Wit *et al.*[10] As is shown in Ref. 10 we can describe the intensity distribution of the mth transition in the Mössbauer spectrum by

$$S(m,\omega) = \mathrm{Re}[\underline{W}(m) \cdot \underline{A}(m)^{-1} \cdot \underline{1}] \tag{4}$$

and the complete Mössbauer spectrum by

$$S(\omega) = \sum_m S(m,\omega) \ , \tag{5}$$

where the sum is over the allowed transitions. In these expressions $\underline{1}$ is a column vector of ones, $\underline{W}(m) = C(m)\{p_1, p_2, \ldots, p_{16}\}$, where $C(m)$ is the nuclear transition probability for the mth transition and p_1 to p_{16} are the population densities of the 16 electronic states. The matrix $\underline{A}(m)$ is given by

$$\underline{A}(m) = -\Gamma(m)\underline{I} + i[\underline{\Omega}(m) - \omega \underline{I}] + \underline{\pi} \ , \tag{6}$$

where $\Gamma(m)$ is the halfwidth of the Mössbauer line of the mth transition, $\underline{I}$ the unity matrix, and $\Omega_{kl}(m) = \omega_k(m)\delta_{kl}$ ($k = 1, \ldots, 16$). In the last expression $\omega_k(m)$ is the frequency of the mth Mössbauer transition for given values of $\langle k|J_z|k\rangle$ and $\langle k|J_z^2|k\rangle$, that can be found for all the 16 states with the aid of Eq. (1). Assuming that the Dy electron spin relaxes via the conduction electrons (i.e., through the off-diagonal elements of the s-f interaction,[13] the transition probabilities π_{kl} between the electronic levels are given by

$$\pi(k \to l) = (2k_B D)^{-1} \sum_q |\langle k|J_q|l\rangle|^2 \times \frac{\Delta_{kl}}{\exp(\Delta_{kl}/k_B T) - 1}, \quad E_k < E_l \ ,$$

$$\pi(l \to k) = (2k_B D)^{-1} \sum_q |\langle k|J_q|l\rangle|^2 \times \frac{\Delta_{kl}}{1 - \exp(-\Delta_{kl}/k_B T)}, \quad E_k > E_l \ ,$$

$$\pi(k \to k) = -\sum_{l \neq k} \pi(k \to l) \ , \tag{7}$$

with $\Delta_{kl} = |E_k - E_l|$ and where $\sum_q$ denotes a sum over J_+, J_-, and J_z. If the s-f interaction is written

$$H_{sf} = -(g_J - 1) J_{sf} \vec{J} \cdot \vec{s} \tag{8}$$

the Korringa-like constant D is given by

$$D^{-1} = \left(\frac{\pi}{\hbar}\right)[(g_J - 1) J_{sf} \eta]^2 k_B \frac{K(\alpha)}{(1-\alpha)^2} \ , \tag{9}$$

with g_J is the Landé factor, J_{sf} is the coupling constant between the $4f$-electron spin and the conduction electrons, η is the conduction-electron density of states per one spin direction at the Fermi level, and the factor $K(\alpha)/(1-\alpha)^2$ allows for exchange enhancement of the conduction electrons.[20]

III. EXPERIMENTAL

The sources used for the experiments were obtained by irradiating 12 mg of Gd_2O_3, enriched to 98 at.% in ^{160}Gd, for 5 d in a thermal neutron flux of $2 \times 10^{14} n\ \mathrm{cm}^{-2}\mathrm{s}^{-1}$ in the reactor of the Energie Centrum Nederland (E.C.N.) in Petten. The desired activity ^{161}Tb ($T_{1/2} \simeq 7$ d) is the decay product of ^{161}Gd ($T_{1/2} \simeq 4$ min). ^{161}Tb was separated from the irradiated oxide using the Groningen Isotope Separator and implanted with an energy of 112 keV into an Ag single crystal of purity 99.999% cut perpendicular to the $\langle 111 \rangle$ axis. During the implantation the Ag crys-

tal was kept at liquid-helium temperature. Before the implantation the crystal was etched by a mixture of NH_4OH and H_2O_2 and checked by the Laue method. In order to avoid vapor condensation on the target crystal surface before implantation the target was kept at room temperature during the cooling down of the cryostat until the implantation was started. The average implantation depth is much larger than the thickness of the condensed layer. Using the data of Winterbon,[14] a mean penetration depth of 160 Å and a width of the semi-Gaussian depth distribution of 175 Å can be estimated for Tb in Ag. The implanted dose was 1×10^{14} atoms cm^{-2}, corresponding to a maximum impurity concentration of 500 ppm.

After transportation of this source at liquid-nitrogen temperature, Mössbauer-effect measurements on the 25.7-keV $\frac{5}{2}^- \rightarrow \frac{5}{2}^+$ transition in ^{161}Dy were performed in another cryostat. Magnetic fields were produced by a superconducting split coil. The magnetic field was oriented along the $\langle 111 \rangle$ direction of the crystal. The single-line absorber (11.2 mg cm^{-2} $^{161}DyF_3$) was moved sinusoidally at room temperature with a frequency of 37 Hz. Velocity calibration was performed by means of the moiré technique.[15] Gamma rays were detected with a Kr-CO_2 filled proportional counter. Measurements were performed in magnetic fields of 1.52 and 2.22 T at 1.7 K and of 3.21 T at 4.2 K.

IV. RESULTS AND ANALYSIS

If a rare-earth ion is implanted into a metal it can occupy a substitutional or a nonsubstitutional position in the (cubic) host lattice.[10] In the case of fcc metals the occupation of the substitutional site will be highest after liquid-helium temperature implantation[16,17] because defects are largely frozen in. The $(2J+1)$-fold degeneracy of the electronic ground state of the ion is lifted in different ways for both sites.

The ground state of the substitutional ion is split by two interactions in this case: the Zeeman interaction and the cubic CEF [Eq. (1)]. The second interaction in general leads to a reduction of the hyperfine field and quadrupole splitting as has been discussed.

If a nonsubstitutional ion is associated with damage (e.g., a vacancy) in the host lattice, it is very likely that there is a strong axial component of the CEF. Since Dy^{3+} is a Kramers ion, its ground state will be split into doublets.[9] These doublets are split by the external magnetic field.

The Mössbauer spectra, which are given in Fig. 1(a), show the presence of at least two components, one of which (55%) is associated with Dy ions in a substitutional site (cubic symmetry), while the other one (45%) is associated with Dy ions in a strong axial CEF (with lowest energy state a doublet with $\langle J_z \rangle = \pm J$). This was verified at $B_{ext} = 0$ where the substitutional component shows up as a relaxation broadened single line, whereas the nonsubstitutional component is not affected at all. For this component the line intensities and positions do not depend on B_{ext} so that the axial CEF must be so strong that an isolated doublet $\langle J_z \rangle = \pm\frac{15}{2}$ lies lowest.

Disregarding relaxation effects, the Mössbauer spectrum of ^{161}Dy is the sum of 16 Lorentzians, given by the Hamiltonian:

$$H = -g_N \mu_N B_{hf} \left(\frac{g_N^*}{g_N} I_z^* - I_z^* \right) + \tfrac{1}{4} e^2 q Q \left(\frac{Q^*}{Q} \frac{3I_z^{*2} - I^*(I^*+1)}{I^*(2I^*-1)} - \frac{3I_z^2 - I(I+1)}{I(2I-1)} \right) . \quad (10)$$

The relative areas of the 16 Lorentzians are given by the appropriate Clebsch-Gordan coefficients, multiplied by a factor that depends only on the angle between the magnetic field at the nucleus and the direction in which the γ quanta are detected. The values $g_N^*/g_N = -1.236$ and $Q^*/Q = 1.00$ were used in fitting the spectra.[18]

Because for the substitutional component the magnetic hyperfine field and the direction in which the γ quanta are detected are parallel, the intensity of the $I_z^* - I_z = 0$ transitions is zero and the spectrum is a sum of ten Lorentzians.

For the nonsubstitutional site the direction of the magnetic field at the nucleus is random relative to that of the γ quanta, so the spectrum of this component consists of 16 Lorentzians, the positions of which can be found from Eqs. (2), (3), and (10) by taking $\langle J_z \rangle = \frac{15}{2}$.

The computer fits could be improved by incorporating a spread in the magnetic hyperfine field or in the quadrupole interaction of the substitutional component, which allows for a spread of the CEF parameters, e.g., small deviations from cubic symmetry. Probably there is a spread in both, but it is not possible to determine the spread in the magnetic interaction and quadrupole interaction independently, so a spread in either one of the two is allowed. The parameters derived in fitting the Mössbauer spectra are not influenced by the choice of one of these two ways of fitting. The results of these fits are given in Table I. From these fits the ratios R_M and R_Q given by Eqs. (2b) and (3b) can be calculated. These ratios and the ratios calculated from the best CEF parameters $A_4\langle r^4 \rangle = -13.5$ K and $A_6\langle r^6 \rangle = +5.7$ K are shown in Fig. 2 and Table II. In Table II the ratios R_M and R_Q are also given when no spread in the in-

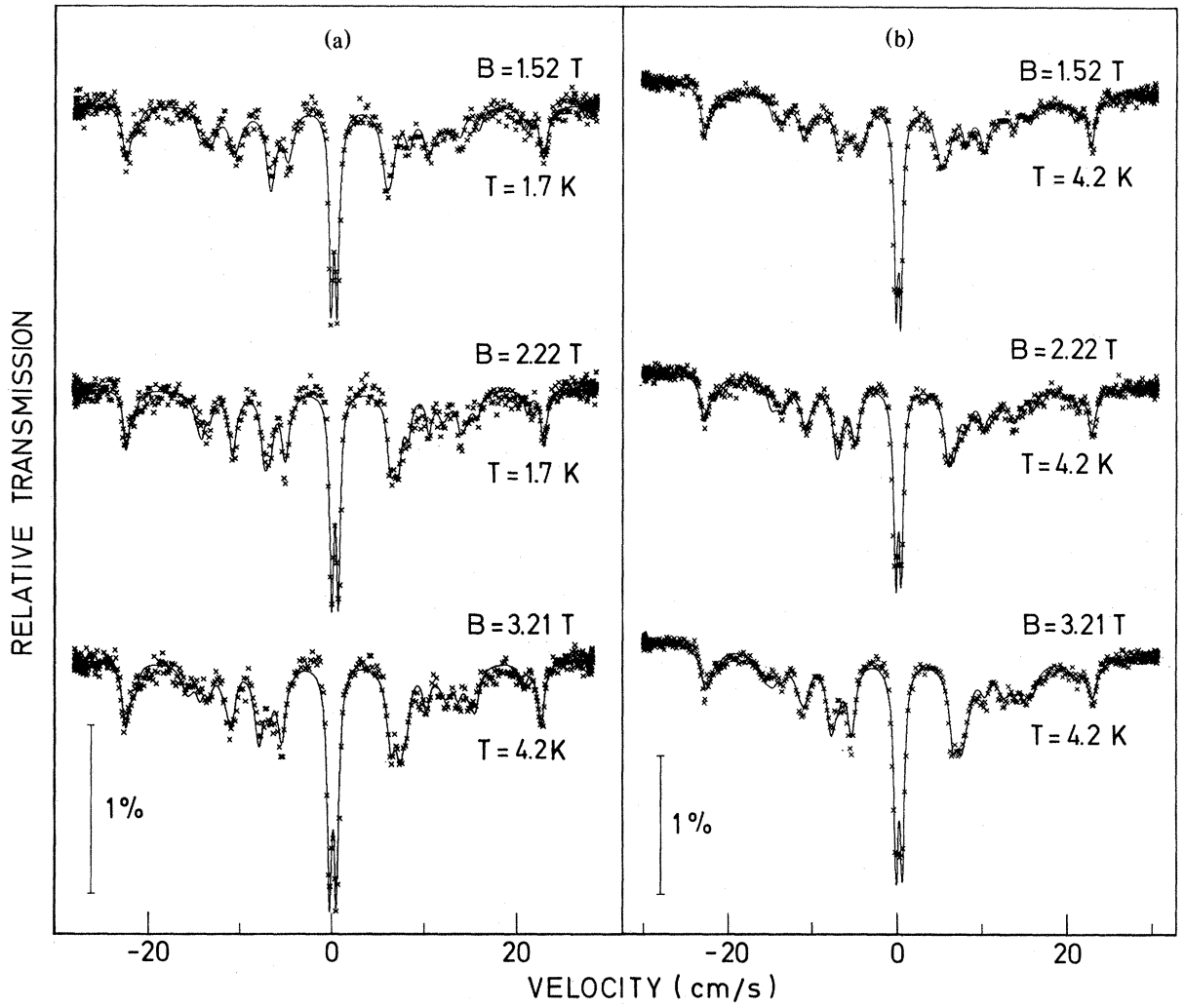

FIG. 1. (a) Mössbauer spectra from ^{161}Dy*Ag* in different magnetic fields at 1.7 and 4.2 K, fitted assuming that only the lowest electronic level is populated. (b) Mössbauer spectra from ^{161}Dy*Ag* in different magnetic fields at 4.2 K, fitted including relaxation phenomena.

TABLE I. Parameters derived in fitting Mössbauer spectra.

B_{ext} (T)	Nonsubstitutional component		Substitutional component		
	$g_N\mu_N B_{hf}$ (cm/s)	$\frac{1}{4}e^2qQ$ (cm/s)	$g_N\mu_N B_{hf}$ (cm/s)	$\frac{1}{4}e^2qQ$ (cm/s)	Relative spread
1.52(2)	4.051(5)	2.50(4)	2.636(13)	0.95(5)	0.71(9)
2.22(2)	4.058(4)	2.66(3)	2.898(9)	1.26(3)	0.36(8)
3.21(3)	4.058(4)	2.58(3)	3.066(8)	1.48(3)	0.33(7)

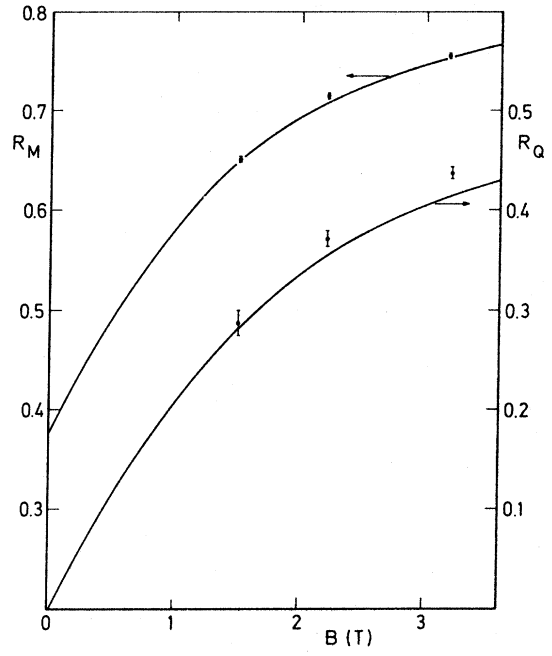

FIG. 2. Measured ratios R_M and R_Q and calculated curve, using $A_4\langle r^4\rangle = -13.5$ K and $A_6\langle r^6\rangle = 5.7$ K, for DyAg as a function of the external magnetic field.

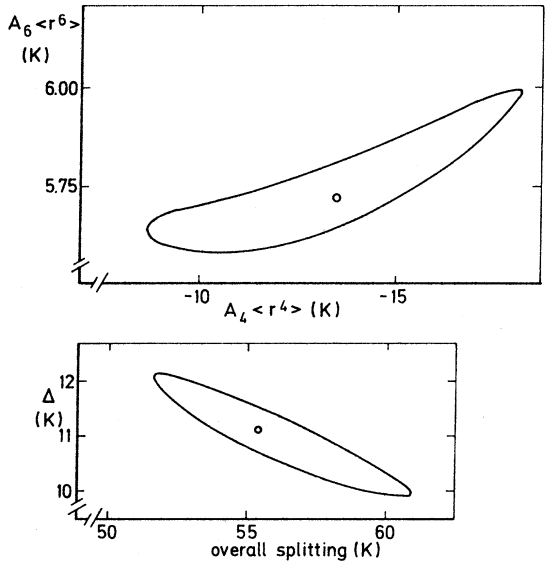

FIG. 3. (a) Allowed values for the crystal-field parameters $A_4\langle r^4\rangle$ and $A_6\langle r^6\rangle$ for DyAg. (b) Allowed values for the separation of the Γ_7 ground state from the Γ_8 excited state and the overall multiplet splitting for DyAg.

teraction is allowed. As can be seen these ratios are not much influenced. Because of their much higher accuracy only R_M has been used for the fit. Figure 3 shows the region of values of $A_4\langle r^4\rangle$ and $A_6\langle r^6\rangle$ that give acceptable fits to the data. In our analysis we have only taken into account statistical errors and we have used as a realistic criterion an increase of χ^2 by a factor of $(\nu+1)/\nu$, in which ν is the number of degrees of freedom. In this figure the region of values of Δ and the overall splitting is also indicated.

Figure 4 shows the calculated energy-level scheme for applied fields from 0 to 3.5 T using $A_4\langle r^4\rangle = -13.5$ K and $A_6\langle r^6\rangle = 5.7$ K. As can be seen from this figure the population of excited electronic states can be neglected at 1.7 K and for $B = 3.21$ T, so that relaxation effects will have no influence on the Mössbauer spectra taken at that temperature.

We also did experiments with ⟨111⟩ single crystals at 4.2 K. The experimental details are the same as described above. The experimental results could not be analyzed satisfactorily in terms of a static hyperfine interaction. This is so because the lowest three

TABLE II. Ratios R_M and R_Q derived experimentally and calculated from CEF parameters.

B_{ext} (T)	R_M				R_Q			
	a	b	c	d	a	b	c	d
1.52(2)	0.645(2)	0.650(3)	0.650	0.603	0.289(7)	0.287(12)	0.282	0.240
2.22(2)	0.710(1)	0.715(2)	0.708	0.655	0.377(6)	0.372(7)	0.353	0.294
3.21(3)	0.754(1)	0.756(2)	0.755	0.699	0.435(5)	0.436(6)	0.414	0.339

[a]No spread in parameters allowed.
[b]Spread in parameters allowed.
[c]Calculated using the CEF parameters found in this paper.
[d]Calculated using the CEF parameters of Ref. 2.

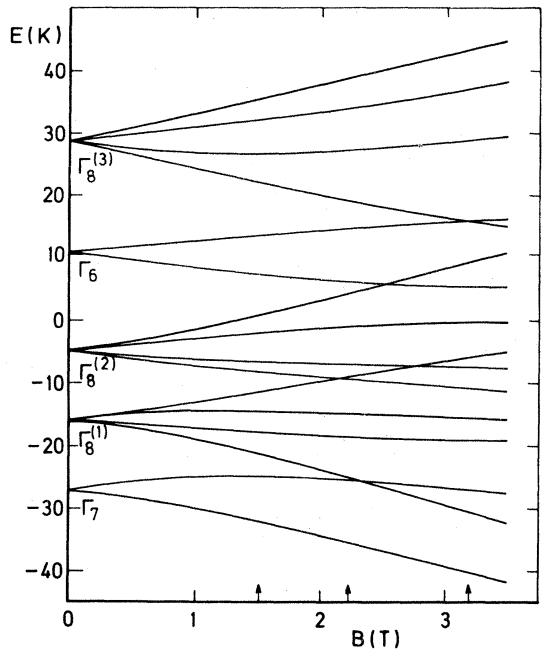

FIG. 4. Electronic energy-level scheme for Dy*Ag* as a function of the magnetic field, calculated using $A_4\langle r^4\rangle = -13.5$ K and $A_6\langle r^6\rangle = 5.7$ K. The three values of the magnetic field, at which measurements have been done, are indicated.

levels are now populated to some extent (Fig. 4), giving rise to relaxation phenomena. These can be treated with the model described earlier. Because only the lowest three levels have to be considered, the dimension of the matrices involved reduces from 16 to 3, so that calculations can easily be performed. The Mössbauer spectra measured at 4.2 K are shown in Fig. 1(b). The solid curves in this figure were calculated as follows. Using the values $A_4\langle r^4\rangle = -13.5$ K and $A_6\langle r^6\rangle = +5.7$ K, all relevant expectation values and energy differences entering in the relaxation model were calculated. Then the relaxation spectrum of the substitutional component was calculated, taking for $\Gamma(m)$ in Eq. (6) the value found from the 1.7 K spectra. This calculated spectrum was fitted to the experimental data with only the intensity as a free parameter, together with the spectrum of the nonsubstitutional component as described before. All parameters that determine this nonsubstitutional spectrum were free in the fit. Several trial values of the relaxation constant D have been used for these fits. The best result was obtained for $(2k_BD)^{-1} = 40(10)$ MHz, about two times larger than the value calculated using Eq. (9) and the ESR linewidth data in Ref. 2. Considering the differences in sample preparation, Dy concentration, and measuring technique, the agreement is quite satisfactory.

V. DISCUSSION

A. Comparison with other experimental data

The first measurements on crystal-field effects in DyAg were performed by Williams and Hirst.[1] From susceptibility measurements they found $A_4\langle r^4\rangle = -70$ K and $A_6\langle r^6\rangle = 13$ K, at variance with our results. Even though they did not observe any deviation from a Curie law, they gave a set of crystal-field parameters for DyAg that is frequently referred to in the literature. They argued that the CEF parameters should not vary much for different rare-earth ions in a given host, in accordance with expectations for a simple point-charge model. Therefore, they used the values derived for ErAg, which does show a clear deviation from a Curie law, also for DyAg. This procedure is not justified, since one can show that a Curie law dependence can be obtained also for quite different values of the CEF parameters. For instance, for our values of the CEF parameters and in the magnetic field applied by Williams and Hirst, no deviations from a Curie law occur, except at very low temperatures.

The first report of ESR measurements on DyAg is by Davidov *et al.*[5] In their analysis they used the overall splitting of 157 K, given but never really measured by Williams and Hirst. Based on this value they report a value between 5 and 10 K for the separation Δ between the ground and first excited level.

Later Oseroff *et al.*[2] reported measurements of the temperature dependence of the static susceptibility and of electron-spin resonance for the systems DyAg and ErAg. They showed that the results of the experiments could be analyzed in terms of a Γ_7 ground state separated from a Γ_8 excited state by $\Delta = 11.5 \pm 1$ K and an overall splitting of 160 ± 25 K for the case of DyAg (or $x = 0.53 \pm 0.01$). These parameters lead to values for the ratio R_M of 0.60, 0.66, or 0.70, and for the ratio R_Q of 0.240, 0.29, or 0.34, respectively. This disagrees with our results from the Mössbauer spectra (Table II). We will show now that these measurements can also be analyzed in terms of an overall splitting of 55.5 K. First we point out that in magnetization measurements one calculates the zero-field susceptibility per ion and one measures the susceptibility per gram so that the concentration of the solute enters into the analysis. Consequently the error in the concentration determination has to be taken into account.

Figure 5 shows the magnetization curve calculated with $\Delta = 11.5$ K and an overall splitting of 160 K. This curve represents also the magnetization data for the 220 ppm alloy of Oseroff *et al.*[2] Their 3% error bars are indicated. Also shown is a magnetization curve for $\Delta = 11.2$ K and an overall splitting of 55.5 K, as found from our experiments. This curve fits

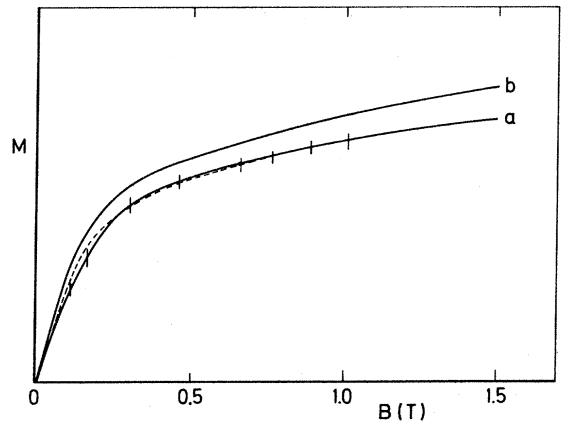

FIG. 5. Magnetization as a function of magnetic field at $T=0.42$ K calculated using $\Delta=11.5$ K and an overall splitting of 160 K (curve a) and using $\Delta=11.2$ K and an overall splitting of 55.5 K (curve b) for a concentration of 220 ppm Dy in Ag. Also indicated is the magnetization curve calculated using $\Delta=11.2$ K and an overall splitting of 55.5 K for a concentration of 200 ppm (dashed curve). Magnetization data from Ref. 2.

the experimental data equally well if we assume a concentration of 200 ppm instead of 220 ppm, as is indicated by the dashed curve. This 10% difference is, according to Ref. 2, within the error bars of the concentration determination. We conclude that the authors of Ref. 2 have highly underestimated the errors in the CEF parameters obtained, because they did not include the concentration inaccuracy.

Figure 6 gives the zero-field susceptibility data with the same kind of curves as for the magnetization.

Oseroff *et al.*[2] have also measured the variation of the g value as a function of angle between the applied dc field and the sample crystal axes at a frequency of 35 GHz (Fig. 7). The curves give the calculated variation using their CEF parameters (curve a) and ours (curve b). As one can see the agreement, although not optimal, is still reasonable in the case of curve b.

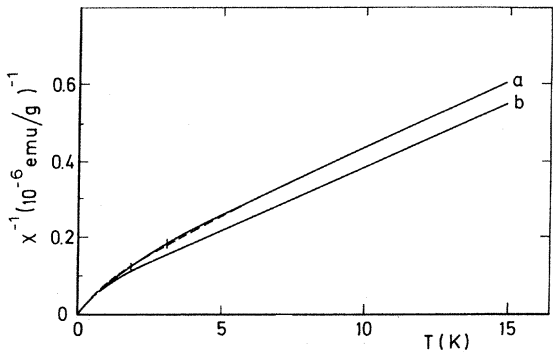

FIG. 6. Reciprocal of the zero-field susceptibility as a function of temperature. Same type of curves as in Fig. 5.

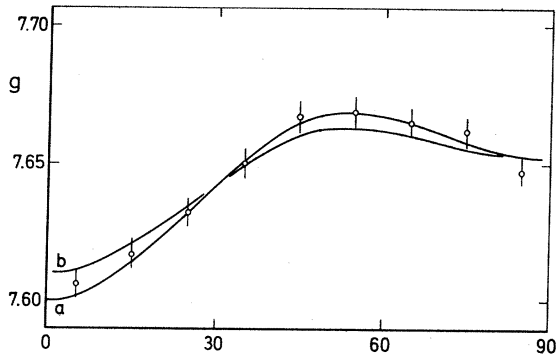

FIG. 7. Variation of the g value vs angular orientation of the applied dc field to the sample axis at a frequency of 35 GHz. The normal to the crystal is ⟨110⟩. Same type of curves as in Fig. 5.

Since most of their other experimental results are less sensitive to the CEF parameters, we do not compare all of them in this paper. It suffices to say that in all cases a very good agreement can be found.

Also specific-heat experiments have been carried out for the system DyAg by Parker *et al.*[3] The CEF parameters as given in this paper can account for the measured Schottky effect but they are rejected on the basis of the other experimental data, notably Ref. 2.

From this discussion it should be clear that in the case of Dy*Ag* Mössbauer-effect measurements in external magnetic fields yield much more accurate CEF parameters than the other techniques, particularly because the Mössbauer spectra are sensitive not only to Δ but also to the position of the other levels in the ground-state multiplet.

B. Discussion of the new results

From the measured values of $A_4\langle r^4\rangle$ and $A_6\langle r^6\rangle$ a Γ_7 ground state follows and from the energy-level diagram we calculate an effective g value, $g=\Delta E/\mu_B B=7.576(5)$, where ΔE is the distance between the lowest two electron states in a field B (used in the ESR X-band measurements). The difference between this value and the measured values, $g=7.66(5)$ (Ref. 5) and $g=7.66(3)$ (Ref. 2), is attributed to a ferromagnetic coupling between the $4f$-electron spin and the conducting electrons. The coupling constant J_{sf} can be calculated using the expression[19]

$$\Delta g = g_{\text{eff}}\left(\frac{g_J-1}{g_J}\right)\frac{J_{sf}\eta}{(1-\alpha)} \quad . \tag{11}$$

Here g_J is the Landé g factor ($\frac{4}{3}$ for Dy), η is the conduction electron density of states per one spin direction at the Fermi level, and the factor $(1-\alpha)^{-1}$

defined in Ref. 20 allows for exchange enhancement of the conduction electrons [see also Eq. (9)]. The value of α can be obtained from Matzkanin *et al.*[21]: $\alpha = 0.76$. The value of η can be found from specific-heat measurements using MacMillan's relation[22]

$$\gamma_e = \tfrac{2}{3}\pi^2 k_B^2 \eta (1+\lambda) \ , \tag{12}$$

where λ is the electron-phonon mass enhancement. In the case of Ag, λ should be very small (no superconductivity observed). Reported values of γ_e range from 0.61 to 0.74 mJ mole^{-1} K^{-2}.[3,23,24] This yields, according to Eq. (12), $\eta = 0.07$ states/eV atom spin. Using this value, the coupling constant J_{sf} is calculated to be $J_{sf} = 0.16(5)$ eV. This is much lower than in Ref. 2, because we calculated J_{sf} including some enhancement factors. Using the same enhancement factors we find from the ESR linewidth data in Refs. 2 and 5 a value of $J_{sf} = 0.17(3)$ eV, in nice agreement with the value given above.

The CEF results can be compared with theoretical calculations. Using a lattice-sum point-charge calculation, assuming an effective charge $+|e|$, one obtains for the CEF parameters $A_4\langle r^4\rangle = 31.4$ K and $A_6\langle r^6\rangle = 4.9$ K using the Herman and Skillman free-atom wave functions.[25] These values have been corrected for an enhancement of the lattice-sum CEF parameters when overlap with nearest neighbors is taken into account.[26] Within the large uncertainty of the calculated $\langle r^n\rangle$, the point-charge value for $A_6\langle r^6\rangle$ does not disagree with the value obtained experimentally. However, $A_4\langle r^4\rangle$ has even changed sign with respect to the point-charge value. To account for this we refer to a paper of Dixon and Dupree,[26] where the effect of the conduction electrons has been studied. These authors used an orthogonalized plane wave (OPW) to describe the conduction-electron wave function and considered the effect of mixing f and d character into the conduction-electron wave function for the case of rare-earth noble-metal alloys. In doing this, they assumed the conduction electrons to be noninteracting and independent, with two $6s$ and one $4f$ electron entering the conduction band. One might therefore expect the conduction electrons to possess a small amount of the spatial character of this $4f$ orbital. The method includes also the contribution from the $5d$ character of the conduction electrons. This d character must be included when an unoccupied $5d$ orbital lies fairly close to the Fermi level. The change in sign of $A_4\langle r^4\rangle$ observed in many alloys[1] is ascribed to this.

In the calculations the conduction-electron wave function was made orthogonal to all the $4f$ orbitals (occupied and unoccupied) and all core states of a rare-earth ion and its immediate neighbors. To correct for the fact that the $4f$ shell is actually not completely occupied, the authors[26] admixed an amount ϵ_f of one of the unoccupied $4f$ states in the conduction-electron wave function. In the same way ϵ_d is a parameter to incorporate $5d$ character in this wave function.

Using their calculations one can determine the parameters ϵ_d and ϵ_f from the CEF parameters obtained experimentally. This yields $\epsilon_f = -0.08(4)$ and $\epsilon_d = 0.035(2)$. The errors given are determined by the uncertainties in the experimental values of $A_4\langle r^4\rangle$ and $A_6\langle r^6\rangle$. However, as there is considerable uncertainty in the wave functions, the real errors are much larger. ϵ_f is very much influenced by this uncertainty, while ϵ_d is rather insensitive. These values cannot be compared very well with the values obtained for other rare-earth silver-based alloys, because no accurate results are available. For comparison, we therefore give values derived from our accurate results for Dy*Au* (Ref. 27): $\epsilon_f = 0.30(1)$ and $\epsilon_d = -0.036(1)$ using Herman and Skillman wave functions. We see that the mixing parameters ϵ_d are roughly equal in Dy*Au* and Dy*Ag*, while ϵ_f is too uncertain to draw any conclusion.

In order to understand the systematics of these values, accurate and reliable experimental values for $A_4\langle r^4\rangle$ and $A_6\langle r^6\rangle$ in a number of systems (especially, in systems with varying conduction-electron densities) are needed. We have already performed Mössbauer measurements in external fields on the systems Dy*Al*,[17] Dy*Cu*,[28] Dy*Au*,[27] and Dy*Mo*. It should be noted that ^{169}Tm as a solute also presents an excellent case for determining CEF parameters in dilute metal alloys by our method.

ACKNOWLEDGMENT

The authors thank Mr. J. J. Smit for performing the radioactive implantations.

[1] G. Williams and L. L. Hirst, Phys. Rev. 185, 407 (1969).
[2] S. Oseroff, M. Passeggi, D. Wohlleben, and S. Schultz, Phys. Rev. B 15, 1283 (1977).
[3] F. T. Parker, H. Oesterreicher, and H. Eno, Phys. Rev. B 16, 4382 (1977).
[4] H. Happel, P. v. Blanckenhagen, K. Knorr, and A. Murani, in *Crystal Field Effects in Metals and Alloys*, edited by A. Furrer (Plenum, New York, 1977).
[5] D. Davidov, C. Rettori, A. Dixon, K. Baberschke, E. P. Chock, and R. Orbach, Phys. Rev. B 8, 3563 (1973).
[6] S. Oseroff and L. Calvo, Phys. Rev. B 18, 3041 (1978).
[7] M. T. Hutchings, Solid State Phys. 16, 227 (1964).

[8]K. R. Lea, M. J. M. Leask, and W. P. Wolf, J. Phys. Chem. Solids 23, 1381 (1962).
[9]A. Abragam and B. Bleaney, *Electron Paramagnetic Resonance of Transition Ions* (Clarendon, Oxford, 1977).
[10]H. P. Wit, L. Niesen, and H. de Waard, Hyper. Inter. 5, 233 (1978).
[11]Y. Berthier, J. Barak, and B. Barbara, Solid State Commun. 17, 153 (1975).
[12]I. Nowik, Phys. Lett. A 24, 487 (1967).
[13]J. Kondo, Solid State Phys. 23, 183 (1968).
[14]K. B. Winterbon, *Ion Implantation Range and Energy Deposition Distributions* (IFI/Plenum, New York, 1975), Vol. II.
[15]H. de Waard, Rev. Sci. Instrum. 36, 1728 (1965).
[16]H. P. Wit, N. Teekens, L. Niesen, and S. A. Drentje, Hyper. Inter. 4, 674 (1978).
[17]P. J. Kikkert and L. Niesen, J. Phys. (Paris) 41, C1-203 (1980).
[18]R. L. Cohen and K. W. West, in *Hyperfine Interactions in Excited Nuclei,* edited by G. Goldring and R. Kalish (Gordon and Breach, New York, 1971), p. 613.
[19]K. Yosida, Phys. Rev. 106, 893, 107 (1965).
[20]T. Moriya, J. Phys. Soc. Jpn. 18, 512 (1965).
[21]G. A. Matzkanin, J. J. Spokas, C. H. Sowers, D. O. van Ostenberg, and H. G. Hoeve, Phys. Rev. 181, 559 (1969).
[22]W. L. MacMillan, Phys. Rev. 167, 331 (1967).
[23]D. L. Martin, Phys. Rev. 141, 576 (1966).
[24]B. A. Green and H. V. Culbert, Phys. Rev. 137, 1168 (1965).
[25]F. Herman and S. Skillman, *Atomic Structure Calculations* (Prentice-Hall, Englewood Cliffs, N.J., 1963).
[26]J. M. Dixon and R. Dupree, J. Phys. F 3, 118 (1973).
[27]P. J. Kikkert and L. Niesen, J. Phys. F (to be published).
[28]P. J. Kikkert and L. Niesen, Hyper. Inter. 8, 135 (1980).